Direct and indirect impact of the bacterial strain Pseudomonas aeruginosa on the dissolution of synthetic Fe(III)- and Fe(II)-bearing basaltic glasses

Anne Perez, Stéphanie Rossano, Nicolas Trcera, Aurélie Verney-Carron, Céline Rommevaux, Chloé Fourdrin, Ana Carolina Agnello, David Huguenot, François Guyot

Direct and indirect impact of the bacterial strain *Pseudomonas aeruginosa* on the dissolution of synthetic Fe(III)- and Fe(II)-bearing basaltic glasses

Anne Perez [a,*], Stéphanie Rossano [a,*], Nicolas Trcera [b], Aurélie Verney-Carron [c], Céline Rommevaux [d], Chloé Fourdrin [a], Ana Carolina Agnello [a,e], David Huguenot [a], François Guyot [f]

[a] *Université Paris-Est, Laboratoire Géomatériaux et Environnement, (EA 4508), UPEM, 77454 Marne-la-Vallée, France*
[b] *Lucia Beamline, Synchrotron SOLEIL, 91192 Gif-sur-Yvette, France*
[c] *Laboratoire Interuniversitaire des Systèmes Atmosphériques, UMR CNRS 7583 / UPEC / UPD, IPSL, 94010 Créteil, France*
[d] *Aix Marseille Univ., Université de Toulon, CNRS, IRD, MIO UM 110 , 13288, Marseille, France*
[e] *Research and Development Center for Industrial Fermentations, Calle 50 N°227, B1900AJL La Plata Argentina*
[f] *Institut de Minéralogie, de Physique des Matériaux et de Cosmochimie, Muséum National d'Histoire Naturelle, CNRS, Sorbonne Université, IRD, 75005 Paris, France*

Author to whom correspondence should be addressed:
anne.perez@u-pem.fr (A. Perez)
stephanie.rossano@u-pem.fr (S. Rossano)
Laboratoire Géomatériaux & Environnement
5 boulevard Descartes, 77 420 Champs-sur-Marne

Abstract

This study is dedicated to the determination of the respective direct and indirect bacterial contributions during the dissolution process of synthetic basaltic glass. In this regard, three different types of glasses – with or without Fe, in the reduced Fe(II) or oxidized Fe(III) states – were prepared on the basis of a simplified basaltic glass composition. In order to assess the direct/indirect bacterial contributions, the experimental set-up included the use of dialysis bags, which prevent the direct contact between the model siderophore-producing strain *Pseudomonas aeruginosa* and the synthetic glasses. The glasses were immersed at 25°C and pH 6.5 in a growth medium inoculated with the strain and submitted to alteration times from 8 hours to 6 days. Throughout the dissolution experiments, the following parameters were monitored: determination of bacterial growth, quantification of siderophore (*i.e.* pyoverdine) production, microscopic observation of the glass surface and determination of dissolution kinetics. The results were compared to identical experiments performed without dialysis bags and show different behaviors depending on the accessibility of the cells to the glass. For all compositions, isolating the glass from the bacterial suspension triggered the biosynthesis of siderophores. This production appeared to be either continuous in the Fe-free system or stopped as soon as the bacteria entered their stationary phase of growth in the Fe-bearing systems. By contrast, allowing a direct contact between the glass surface and the bacterial suspension triggered a high and continuous production of siderophore in the Fe-free system and only a small production in the presence of the Fe(II)-bearing glass. The dissolution rates were approximately increased by a factor of 3 for Fe-free and Fe(III)-bearing glass and by a factor of 2 for Fe(II)-bearing glass compared to sterile experiments. Pyoverdine concentrations similar to those obtained with dialysis bags were obtained in presence of the Fe(II)-bearing glass and were below detection limit in presence of the Fe(III)-bearing glass. The dissolution rates were correlated to siderophore concentrations as they increased this time with respect to sterile experiments in the order Fe(III)-bearing glass < Fe(II)-bearing glass < Fe-free glass. Finally, in all experimental cases, the bacteria appeared to increase the dissolution kinetics of the three model glasses involved. However, the Fe(III) accessibility to the bacterial cells was shown to be the key parameter regulating the bacterial activity and their efficiency in accelerating the dissolution.

Key-words:

Basaltic glass; *Pseudomonas aeruginosa*; siderophore; bioalteration; dissolution kinetics

Introduction

Silicate glasses are abundant at the Earth's surface and notably near the oceanic ridge axes where large amounts of lava are emitted every year, generating a profusion of both amorphous and crystalline basaltic rocks. The alteration processes of basaltic glasses in permanent contact with seawater are known for partially controlling the composition of this latter but also the composition of the oceanic crust and impacting on the geochemistry of the Earth mantle. The alteration of basaltic glasses could also have a significant impact on the Earth's climate by contributing to the sequestration of atmospheric CO_2 though carbonation processes resulting from the dissolution of the glass and the release of earth alkali elements (Berner et al., 1983). Understanding the alteration mechanisms of the oceanic crust at low temperatures is thus essential to implement the Earth surface mass-balance studies and then improve the geochemical models predicting the evolution of our planet (Hart, 1970; Staudigel and Hart, 1983; Spivack and Staudigel, 1994; Gislason and Oelkers, 2003).

During the last two decades, the high diversity and the abundance of the microorganisms living at the subsurface of oceanic basalts were evidenced (Thorseth et al., 2001; Santelli et al., 2009; Mason et al., 2009; Orcutt et al., 2011; Henri et al., 2015; Sudek et al., 2017). As basaltic glasses represent one of the most profuse source of Fe and also contain additional elements (Mg, Ca, K…) required for microbial nutrition (Staudigel and Hart, 1983), they are suspected to sustain the development of microbial communities (Sudek et al., 2009). The literature attests to four main potential bacterial sinks for the elements constituting silicate materials submitted to bioalteration: 1/ adsorbed or 2/ incorporated inside the bacterial cells, 3/ trapped within the biofilms or 4/ complexed with bacterial exometabolites such as siderophores (e.g. Uroz et al., 2009). However, the role of basaltic glasses as a substantial source of nutrients, the impact of such microbial activity on their dissolution rates and its potential control on the biogeochemical cycling of elements at the rock/water interface is still a matter of debate (Templeton et al., 2005; Cockell et al., 2010; Henri et al., 2016).

Numerous laboratory studies were dedicated to the understanding of the basaltic glass dissolution processes in a various range of abiotic experimental conditions (e.g. Guy and Schott, 1989; Daux et al., 1997; Techer et al., 2000, 2001; Oelkers, 2001; Oelkers and Gislason, 2001; Stroncik and Schmincke, 2001; Gordon and Brady, 2002; Crovisier et al., 2003; Gislason and Oelkers, 2003; Wolff-Boenisch et al., 2004a; Flaathen et al., 2010; Verney-Carron et al., 2011; Parruzot et al., 2015; Perez et al., 2015). The dissolution of basaltic glass is traditionally defined by two simultaneous mechanisms, whose predominance notably depends on the pH of the aqueous fluid: (1) an ion exchange between network-modifying elements of the glass (Na, K, Ca, Mg) and hydrogenated species from the solution (interdiffusion) and (2) the hydrolysis of the bonds linking oxygen atoms to network-forming elements of the glass (Si, Al, Fe(III)). Dissolution can also be presented as the breaking of all metal-oxygen bonds (from the weakest to the strongest) until the structure is completely destroyed (Oelkers, 2001; Oelkers and Gislason, 2001). As the rate-limiting step of the basaltic glass dissolution process is the detachment of tetrahedral Si near the glass surface, the change of the other network-forming elements

(Al, Fe) speciation is assumed to influence the dissolution rate. For these reasons, the impact of the introduction in the liquid medium of biomolecules known for their high affinity with such cations should be investigated.

Several field studies conducted in deep-sea water and dedicated to the characterization of microbial communities show that if the many cultured organisms are metabolically and functionnaly diverse, they display at least two of the tested functions: heterotrophy, Fe(II) and Mn(II) oxidation and siderophore production (e.g. Sudek et al., 2009). Siderophores are molecules produced when bacteria are submitted to a nutrient stress, and especially to a high need in Fe. The biosynthesis of siderophores involves several steps catalysed by specific enzymes in different locations from cytoplasm to periplasm, from where they are secreted to the extracellular medium (Schalk and Guillon, 2013). Siderophores have generally a very high affinity for two of the three network-forming elements Al and Fe(III). In two previous studies (Perez et al., 2015, 2016), experiments performed on synthetic Fe(II), Fe(III)-bearing basaltic glasses (MORB2, MORB3) and Fe-free glass (HAPLO) in the presence of siderophores and then in the presence of the model siderophore-producing strain *Pseudomonas* (*P.) aeruginosa* exhibited enhanced dissolution rates compared to those performed in sterile controls. The results highlighted the promoting role of organic ligands as complexing agents, and particularly of pyoverdines, which are the siderophores produced by *P. aeruginosa*. These conclusions were in agreement with numerous abiotic studies dealing with dissolution kinetics of minerals/oxides/silicate glasses in the presence of organic molecules (Welch and Ullman, 1992; Watteau and Berthelin, 1994; Stillings et al., 1995; Drever and Stillings, 1997; Kraemer et al., 1999; Liermann et al., 2000; Cocozza et al., 2002; Cheah et al., 2003; Wolff-Boenisch, 2007; Wang et al., 2005; Olsen and Rimstidt, 2008; Martinez-Luevanos et al., 2011; Torres et al., 2014; Akafia et al., 2014; Lazo et al., 2017). This promoting effect is in favour of the occurrence of a bacteria-mediated process, which notably contrasts with several recent studies attesting to a small or negligible impact of the presence of bacteria on dissolution kinetics of minerals (Hopf et al., 2009; Hutchens, 2009; Sverdrup, 2009; Bray et al., 2015) and of basaltic glass (Wolff-Boenisch, 2011; Stockmann et al., 2012). It is therefore important to note that this promoting effect was observed in specific conditions (growth phase and nutrient free systems) in which the acquisition of nutrient was crucial for the bacterial cells. Even though the impact of siderophores on the dissolution kinetics of basaltic model glasses was evidenced, the bacterial-promoted dissolution mechanisms of the glasses remain hard to define as bacteria can also directly interact with glass surfaces or produce other metabolites that could influence the dissolution rates (Ullman et al., 1996; Hutchens, 2009; Shirokova et al., 2012; Ahmed and Holmström, 2015; Cornu et al., 2017; Wang et al., 2018).

The present work aims to decipher direct and indirect dissolution mechanisms of basaltic glass by bacteria. For this purpose, bioalteration experiments were performed on HAPLO, MORB2 and MORB3 synthetic glasses. In order to assess the direct/indirect bacterial contributions, the experimental set-up included the use of dialysis bags, which prevented the direct contact between the model siderophore-producing strain *P. aeruginosa* and the basaltic glasses tested. Throughout the dissolution experiments the following parameters were monitored: determination of bacterial growth, quantification

of siderophore (*i.e.* pyoverdine) production, microscopic observation of the glass surface and determination of dissolution kinetics.

Material and Methods

1. Samples

The theoretical compositions of the three model glasses used in this study are given in Table 1. The MORB2 and MORB3 glasses were prepared according to a simplified typical *Mid Oceanic Ridge Basalt* composition and contain mainly Fe(II) and Fe(III), respectively. The HAPLO glass is an Fe-free equivalent composition in which Fe is mainly substituted by Mg.

Table 1: Nominal compositions of the synthetic Fe(II)-bearing glass (MORB2), Fe(III)-bearing glass (MORB3) and Fe-free glass (HAPLO) of interest.

	MORB2 & 3 (wt %)	**HAPLO** (wt %)
SiO_2	48.6	51.6
Al_2O_3	15.7	16.7
FeO	12.5	0.0
CaO	11.1	11.8
MgO	7.7	15.2
Na_2O	2.7	2.9
TiO_2	1.4	1.5
K_2O	0.2	0.3

MORB2, MORB3 and HAPLO glasses were prepared according to the procedure described in the work of Perez et al. (2016). More details concerning the characterization of these glasses (DRX, XAS, BET measurements) are also given in this previous study.

2. Bioalteration experiments

Freshly grown cultures of *P. aeruginosa* ATCC® 9027 (Sigma Aldrich) bacteria having identical age and initial nutritional status were used in all bioalteration experiments.

Two growth media were used in this study. The bacteria were first grown in 2 mL of Lysogeny Broth (LB) medium, a nutritionally rich medium containing: 10 g L^{-1} tryptone, 5 g L^{-1} yeast extract, 5 g L^{-1} NaCl.

The prepared glasses were then immersed in a buffered (pH 6.5) MM9 medium whose composition was adapted from Schwyn and Neilands (1987) and Liermann et al. (2000). Near neutral conditions of pH were chosen to allow for comparison with similar experiments conducted in abiotic conditions (Perez et al., 2015). The medium composition was as follows: 6.06 g L^{-1} Na_2HPO_4, 0.3 g L^{-1} KH_2PO_4, 0.5 g L^{-1} NaCl, 1.0 g L^{-1} NH_4Cl and 50 mM Bis Tris. The pH was adjusted by adding HCl 1 M. The solutions were sterilised and cooled to 25 °C. They were then supplemented with 0.2% (v/v) 1 M $MgSO_4$ (final concentration 2 mM), 1% (v/v) filter-sterilised (cellulose filter, Ø0.2 µm) 20% (w/v) glucose (final concentration 1 M) and 0.01% (v/v) 1 M $CaCl_2$ (final concentration 0.1 mM); these solutions were prepared and sterilized separately. No Fe was detected in the prepared growth medium and no precipitate formation was observed. Dissolution experiments were performed in sterile borosilicate erlenmeyers closed with cotton plugs to allow free passage of air over the edge of the vessels and to maintain an aerobic aqueous environment. A volume of 250 mL of MM9 6.5 medium was mixed with 0.625 g of glass powder and inoculated together with 125 µL of the LB culture of *P. aeruginosa* after 30 h of incubation at 25 °C and 160 rpm. By contrast with the experiments presented in Perez et al. (2016), the glasses were isolated from the bacterial suspension by sterile dialysis bags (®CelluStep T4). Porous dialysis membranes allow small solutes to pass while large species are retained and can thus effectively be used as a separation process based on size rejection. The Molecular Weight Cut Off of the membranes used in our experiments is 12000-14000 Da, which means that: (1) 90% of the species whose molecular weight ranges between 12000 and 14000 Da do not pass the membrane and do not access to the glass surfaces and (2) 100% of the species whose molecular weight exceeds 14000 g/mol do not pass the membrane. In the context of this study, the used membranes allow most exometabolites, in particular siderophores, to interact with the glass surface whereas the bacteria cells are isolated from the solid samples.

At each dissolution time, 2.3 mL of the liquid medium were filtered (cellulose acetate filter, Ø0.2 µm) and kept for Inductively Coupled Plasma and Optical Emission Spectroscopy (ICP-OES) analysis whereas 1.7 mL were placed in a spectrophotometer cell for Optical Density (OD) measurements and 200 µL were plated right away on LB agar medium for the microbial counting procedure. Sampling times were chosen as a function of the bacteria growth: frequent from the beginning until the end of the exponential phase and then more distant (0.6, 1, 1.6, 2, 3 and 5.7 days). Experiments were extended until 15 days of experiments and 1.7 mL were sampled at days 8, 10, 13 and 15 and introduced in a spectrophotometer cell for additional measurements.

For each glass, sterile experiments (without introducing *P. aeruginosa*) were conducted following the same protocol and are mentioned as “abiotic control” in the Results and Discussion section. Moreover, *P. aeruginosa* was cultivated in identical conditions but without adding the glass into the system. These experiments were mentioned as “control” in the following sections.

All experiments were performed in duplicates.

3. Analysis

The amounts of dissolved Al, Fe and Si were analyzed using a Perkin Elmer Optima 8300 ICP-OES. Measurements were performed using emission wavelength at 288.16 nm (Si), 308.22 nm (Al), 239.56 nm (Fe). Ca, Mg, Na, K were exempted from analysis being initially present in significant amounts in the growth medium.

For each element and at each dissolution time, the normalized mass loss NL*i* from the glass into the solution was calculated using Eq. (1).

$$NL_i = \frac{[i]}{\left(\frac{S}{V}\right)\times x_i} \quad (1)$$

where *[i]* is the concentration (mg L^{-1}) of the element i in solution, S the initial surface of the glass powder in contact with the fluid, V the volume of solution and x_i the mass percentage of the element *i* in the glass.

Considering a linear regression, the initial slope of the curve was calculated in order to evaluate the *apparent* initial rate of dissolution *ri* as given in Eq. (2):

$$r_i = \frac{dNL_i}{dt} \quad (2)$$

At each sampling time, total biomass growth was estimated by measuring the Optical Density (OD) of the incubated medium at 600 nm and by the Colony Forming Unit (CFU) count procedure. After 2.7 days (respectively 2.9 days for MORB3 glass) and 5.7 days, dilutions of the bacterial medium were plated on LB agar and incubated 24 h at 25 °C for the counting step while the sampled solution was also filtered (cellulose acetate filters, Ø0.2 µm) and placed into a spectrophotometric cell. Optical spectra were recorded between 300 and 600 nm. Identical spectrophotometric cells were used for all measurements, with a standard optical path length.

The samples resulting from the dissolution experiments without dialysis bags (see Perez et al. (2016) for the presentation and discussion of the liquid analysis results of these experiments) were dried following a critical point dying (CPD) protocol in order to avoid the damaging effects of surface tension on bacterial cell and biofilm potentially present at the glass surface. 250 µL of glass in suspension in the bacterial medium were mixed with 4 mL of 0,05 M 4-(2-hydroxyethyl)-1-piperazineethanesulfonic acid (HEPES) solution (pH 8) and then slowly injected in a swinnex® containing a polycarbonate filter (Ø 0,22 µm). The glass grains and bacterial cells were retained on the filter and successively washed with 5 mL of 50%, 70%, 96% and 100% ethanol (vol.). The filter was carefully kept in an absolute ethanol bath then introduced in a CPD chamber *(Leica EM CPD300)* and submitted to 20 cycles (CO_2 injection, increase of temperature and pressure and depressurisation) of 4 min each. After being dried,

the samples were immediately carbon coated and observed with Scanning Electron Microscopy (*Zeiss Ultra55* microscope) with a filament tension of 2 kV.

Results and Discussion

1. Bacterial growth and siderophore production

1.1. Growth

Optical densities (ODs) at 600 nm of the sampled solutions are plotted versus time in Figure 1 for the three glasses. For each glass composition, the ODs measured in the presence of dialysis bags (D) are compared to the ODs measured in dialysis-free experiments (Perez et al., 2016). The absorbance of a bacterial medium at 600 nm is correlated to the number of suspended cells within the liquid medium as it characterizes the turbidity of the solution. OD values are in good agreement with the CFU counting. Correlation factors between OD and CFU values have been calculated for each experimental condition and are equal to 0.97 (Control), 0.92 (MORB3), 0.94 (MORB3 D), 0.99 (MORB2), 0.99 (MORB2 D), 0.95 (HAPLO), 0.94 (HAPLO D).

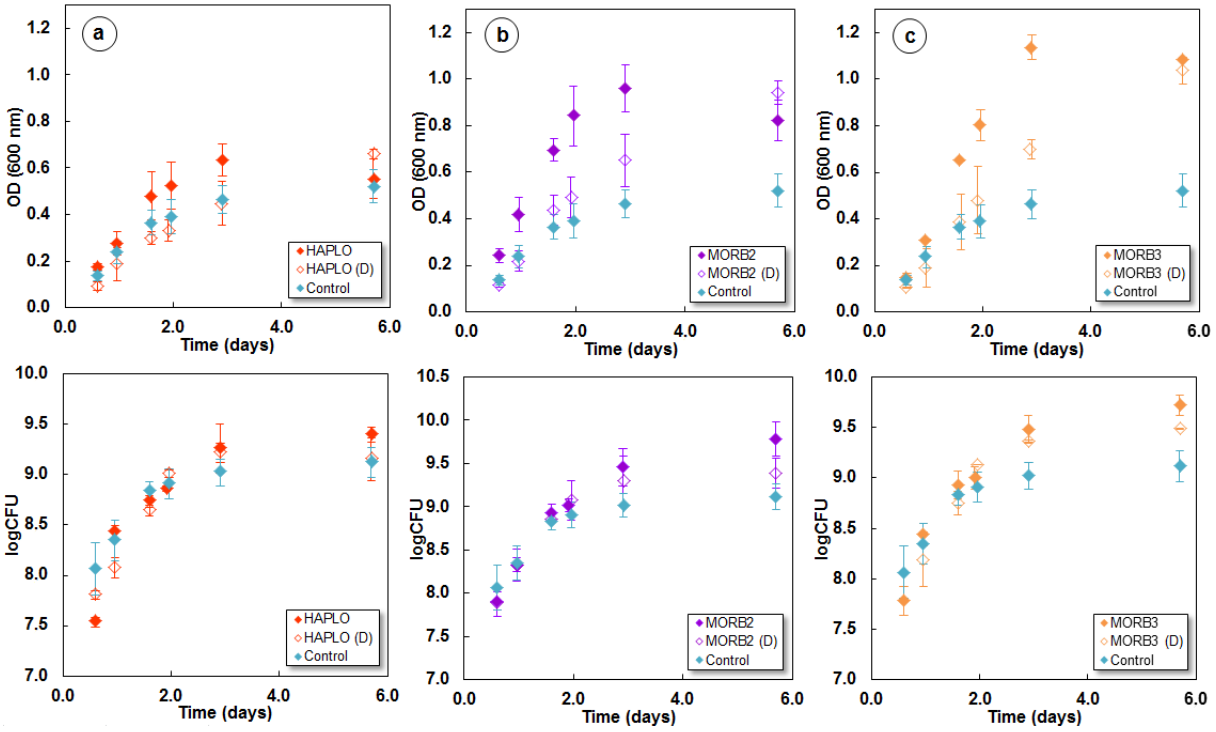

Figure 1: (a) Bacterial growth curves (measured optical densities at 600 nm or Colony Forming Units versus time) of *P. aeruginosa* culture in the presence of the MORB3 (a), MORB2 (b) and HAPLO (d) glasses, confined (empty symbols) or not (full symbols) in dialysis (D) bags. Blue data points represent the control experiment. Growth experiments in MM9 6.5 were performed in duplicates and error bars correspond to ± standard deviation (SD) between the 2 measured values.

The experiments in the presence of the HAPLO glass exhibit growth curves very close to those obtained in the control experiments (Figure 1a). The bacterial growth is more pronounced when bacteria are incubated with Fe-bearing glasses, independently of the presence or absence of dialysis membranes (Figures 1b & 1c). This suggests that Fe-bearing glasses, isolated or not from the bacterial suspension, might represent substantial nutrient sources for *P. aeruginos*a in exponential phase of growth. This result is notably in strong agreement with our previous study (Perez et al. 2016) and with a study by Sudek et al. (2017). In this work, the authors evidenced the elevated growth of *Pseudomonas stutzeri VS 10* incubated in the presence of basaltic samples in comparison with basalt-free experiments.

Moreover, the bacteria concentrations at 5.7 days are similar from one experimental condition (with dialysis) to another (without dialysis). Bacteria concentrations are nevertheless systematically lower in dialysis experiments from 0 to 3 days of incubation, suggesting that isolating the bacterial suspension from the glasses induces a slower cell division process. These results indicate that a direct contact between basaltic glasses and the bacterial suspension favors the bacterial cell division process, possibly as a consequence of an improved nutrient supply. On this point too, our results corroborate the recent findings of Sudek et al. (2017), who observed that a physical contact or at least the proximity of the cells to basaltic samples was correlated to a more pronounced bacterial growth.

The NLs of Fe measured for each duplicate in the cultures incubated in the presence of MORB2 and MORB3 glass (isolated or not from the bacterial suspension by dialysis membranes) are plotted versus time in Figure 2.

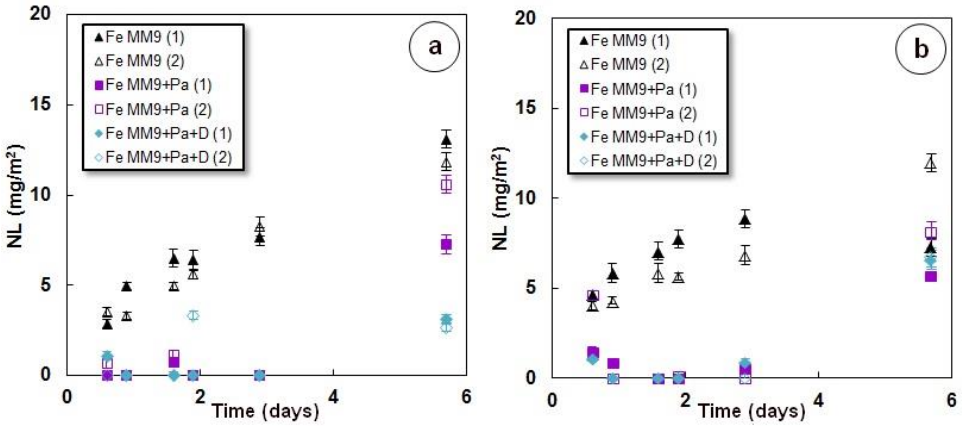

Figure 2: Normalized Loss (NL) profiles of Fe during dissolution experiments of MORB2 (a) and MORB3 (b) glass at 25°C and in the medium MM9 at pH 6.5 in a bacterial culture of *P. aeruginosa* (Pa) isolated (in blue) or not (in purple) from the glass by dialysis bags (D). Open symbols relate to duplicate (1) while full symbol relate to duplicate (2). Black data points represent the NLs measured in sterile controls. Error bars are equal to ± 2SD.

At the difference with dissolution experiments of those same glasses in UPW (Perez et al., 2015), Fe concentration levels in solution are most of the time above the ICP-OES detection limit. Basic speciation calculations (CHESS code) show that, regarding the abundant presence of phosphate salts

303 in the MM9 medium, Fe is mainly present as soluble $FeHPO_4^{+}{}_{(aq)}$, as suggested by Pokrovsky et al.
304 (2009a,b).
305
306 In abiotic conditions (Fe MM9), Fe is continuously released in the medium all along the experiment
307 from both glasses. By contrast, in the presence of the strain (Fe MM9+Pa, Fe MM9+Pa+D), Fe is
308 almost non-detected from 0.6 to 5.7 days independently on the use or not of dialysis membranes. 0.6
309 to 5.7 days also corresponds to a fast cell division step (Figure 1). The few Fe released in solution is
310 probably entirely assimilated by the bacteria and used for the bacterial cell division process. At 5.7
311 days of dissolution experiment, while the bacteria cells are in a stationary phase of growth, Fe is
312 detected in the liquid medium. The presence of Fe at this point shows that Fe is naturally continuously
313 released into the solution, efficiently used by the cells to sustain their growth until they enter a
314 stationary phase and finally remains in solution as it is not needed anymore.
315
316 Coupling bacterial growth and Fe concentrations finally highlights the high-affinity transport
317 mechanisms that *P. aeruginosa* presents in order to acquire Fe. The following section will be
318 dedicated to the identification of the strategies used by the strain to acquire this nutrient.

319 *1.2. Siderophore production*
320
321 Pyoverdines can be detected between 380 and 420 nm with a UV-Vis spectrophotometer through the
322 observation of a two-shoulder characteristic absorption peak (Meyer and Abdallah, 1978). The
323 absorbance spectra of the bacterial cultures, recorded in the UV absorption region characteristic of
324 pyoverdine, are plotted in Figure 3 and compared with the spectra obtained in no dialysis-using
325 experiments.

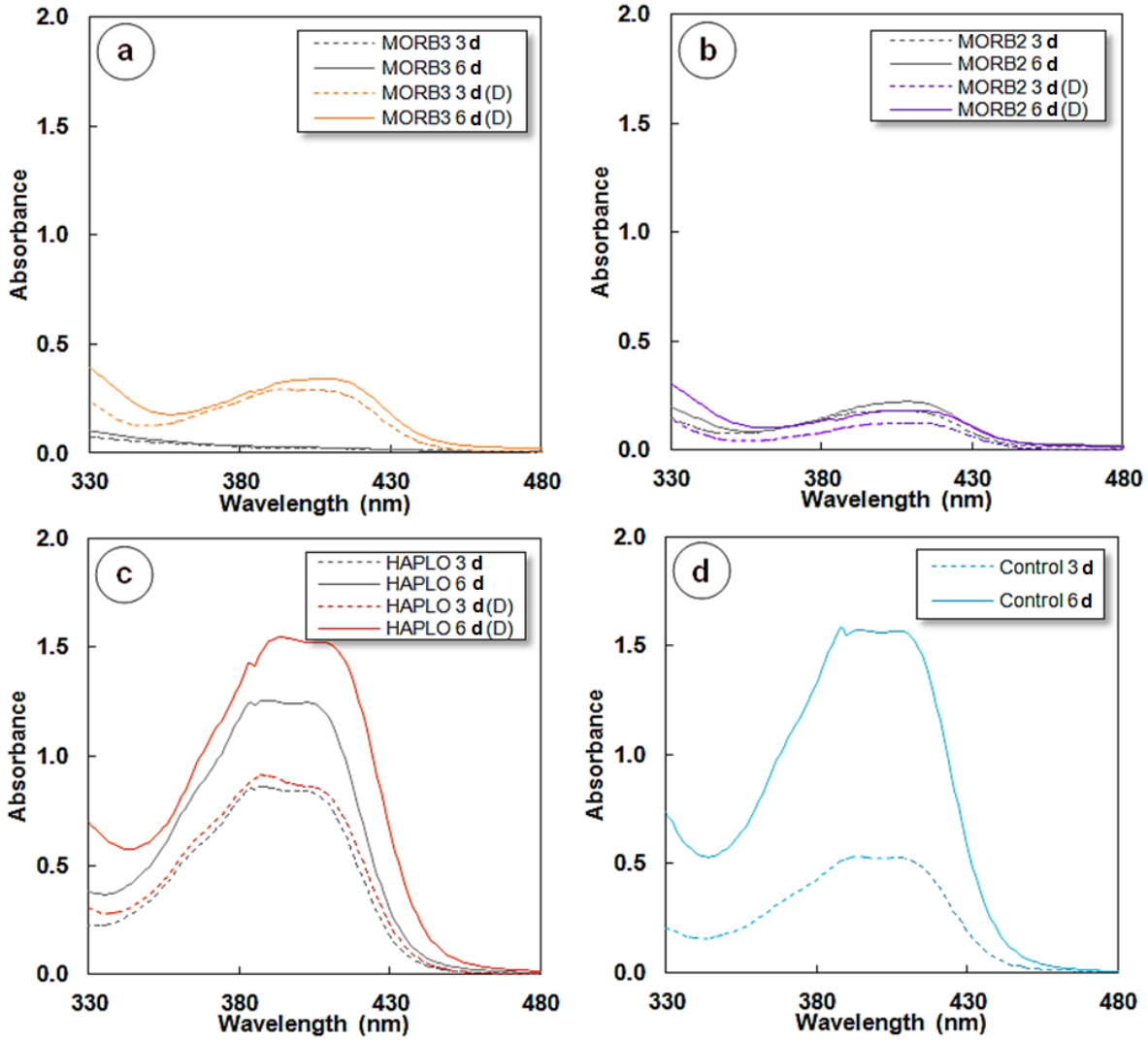

Figure 3: UV Absorption spectra of the MM9 6.5 bacterial medium in the absence (Control) (d) or the presence of the MORB3 (a), MORB2 (b), and HAPLO (c) glasses contained (colored lines) or not (greys lines) in dialysis bags, recorded at 3 days (3d) and 6 days (6d) of the experiments.

According to the shape of the recorded spectra, pyoverdine molecules are detected in all experiments except when bacteria are incubated in contact with the MORB3 glass (no membranes) (Figure 3a).

On the basis of the measured absorbance value at 405 nm (A_{405}), an estimated free pyoverdine concentration can be calculated according to the Beer Lambert law:

$$[PVD] = \frac{A_{405}}{19000} \times 10^6 \qquad (3)$$

The pyoverdine is characterized by different molar extinction coefficients depending on its form in solution. The coefficient of free pyoverdine (19000 L/mol/cm) is lower than that of Fe^{3+}-pyoverdine complexes (26000 L/mol/cm) and greater than that of Al^{3+}-pyoverdine complexes (18000 L/mol/cm). Considering that in our systems, it was not possible to experimentally distinguish between the free pyoverdine, Fe^{3+}-pyoverdine and Al^{3+}-pyoverdine fractions, approximate values of total pyoverdine

concentrations in solution were calculated by using the molar extinction coefficient of free pyoverdine given in Equation (3). These concentrations are plotted in function of the experimental conditions on Figure 4.

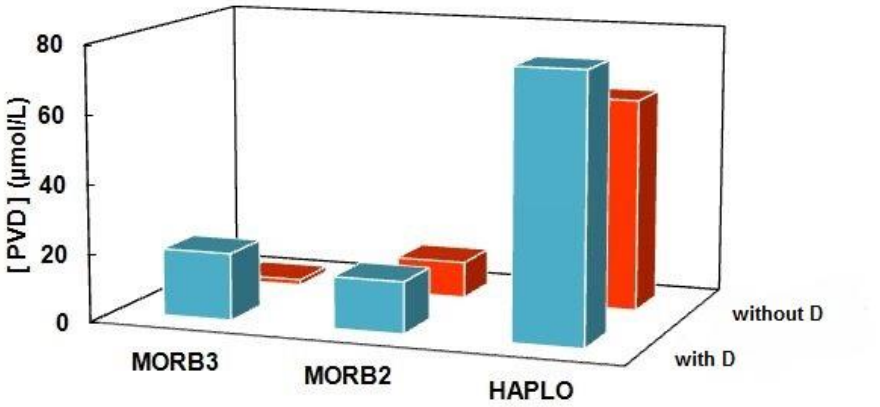

Figure 4: Apparent concentrations in pyoverdine in HAPLO, MORB2 and MORB3 systems after 6 days of experiments with/without dialysis (D) membranes.

In the case of the HAPLO glass (Figure 3c, Figure 4), high amounts of pyoverdine are detected in the incubated medium, independently of the presence or absence of dialysis bags, with pyoverdine concentrations after 6 days greater than or equal to 80 µM and 70 µM, respectively. These results are very close to those obtained in the control experiments (Figure 3d), as both control and HAPLO systems are Fe-free systems.

In the case of the MORB2 glass, the absorbance spectra presented in Figure 3b show similar intensities (corresponding to pyoverdine concentration of ~10 µM, Figure 4) either at 3 and 6 days suggesting that isolating this glass from the bacterial suspension does induce any significant changes regarding the siderophore production. The spectra recorded at days 3 and 6 mainly differ by a change in the shape of the absorption peak of pyoverdine species (Figure 3b). In order to highlight this evolution, more absorbance spectra of the cultures recorded until 15 days of incubation for MORB2 experiments are represented in Figure 5.

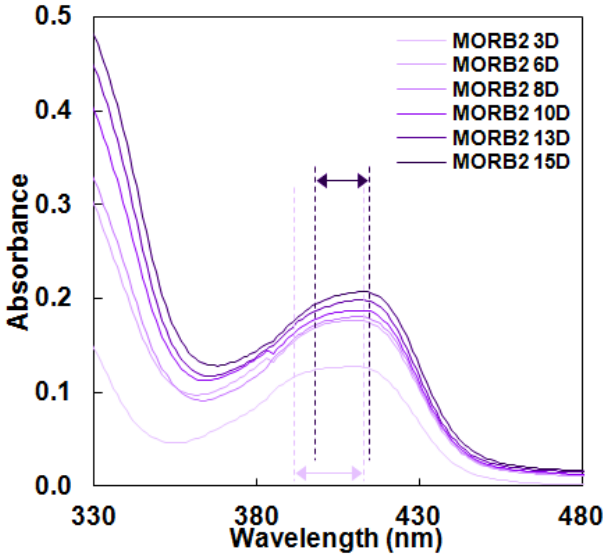

Figure 5: Absorption spectra of the MM9 6.5 bacterial medium in the presence of the MORB2 glass contained in dialysis bags, recorded at 3, 6, 8, 10, 13 and 15 days (D) of the experiments. The arrows materialize the shift of the pyoverdine absorption region toward higher wavelengths with time.

The spectra show a constantly-evolving signal with time (shifted toward higher wavelengths and changing into a one-shoulder peak). At near neutral pH condition, this particular shape characterizes the presence of Fe^{3+}-pyoverdine complexes (Albrecht-Gary et al., 1994). Such an evolution could attest the continuous formation of Fe^{3+}-pyoverdine complexes in solution. The increase in Fe concentration after 5.7 days of MORB2 experiment (Figure 2) was suggesting that no more Fe was incorporated inside the cells once Fe homeostasis conditions were reached. This result shows now that the Fe fraction continuously released from the glass over the course of the experiments (from day 6 to 15) must be, once oxidized into Fe^{3+} in contact with the oxygenated medium, progressively chelated by the free-pyoverdine molecules remaining in solution.

Finally, Figures 3a and 4 show that the presence of dialysis membranes in the MORB3 experiments impacts on siderophore production. If pyoverdine is not detected in the no-dialysis systems, isolating the glass from the bacterial suspension results in a significant production of siderophore in the medium over the course of the experiments. Pyoverdine concentration after 6 days of experiments in the incubated medium is estimated to be lower than or equal to 20 µM. Figure 6 illustrates the change in the shape and the position of the absorption peak of pyoverdine thorough 15 days of experiments.

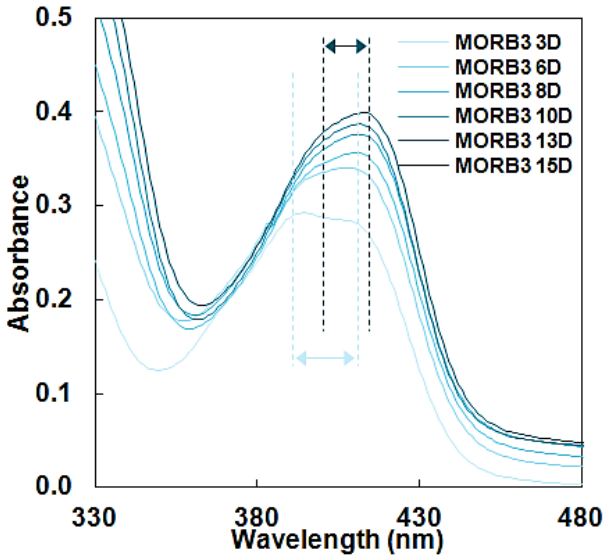

Figure 6: Absorption spectra of the MM9 6.5 bacterial medium in the presence of the MORB2 (a) and MORB3 (b) glasses contained in dialysis bags, recorded at 3, 6, 8, 10, 13 and 15 days (D) of the experiments. The arrows materialize the shift of the pyoverdine absorption region toward higher wavelengths with time.

As observed for the MORB2 glass, the two-shoulder peak characteristic of free-pyoverdine continuously evolve into the single absorption peak of Fe^{3+}-pyoverdine complexes, leading to the same conclusion than those made for the reduced glass.

A previous study performed in identical experimental conditions showed that without any separation between the glass and the bacterial suspension, the Fe fraction abiotically released in solution was lower than the Fe fraction measured within the bacterial cells (Perez et al., 2016). This result suggests that, in the presence of the strain, the Fe fraction naturally released from the glass into the liquid medium is not sufficient to sustain bacterial needs and that, in consequence, more Fe is mobilized from the glass through a non-identified biological process. In the same previous study, the absence of siderophore in the system indicated that pyoverdine molecules were not responsible for enhancing the Fe release. In this work, the results highlight that separating the glass from the bacterial suspension induces a high pyoverdine production by the cells. This production of pyoverdine in presence of dialysis membranes is a good indicator of a high bacterial need in Fe, not observed when the bacteria can access to the glass. This demonstrates that the biological process that enhance the Fe release consists in direct glass surface/bacteria interactions.

1.3. Evidence of direct bacteria/glass interactions

The SEM images of the surface of a MORB3 glass sample incubated in the presence of *P. aeruginosa* without dialysis bags (direct contact) are presented in Figure 7.

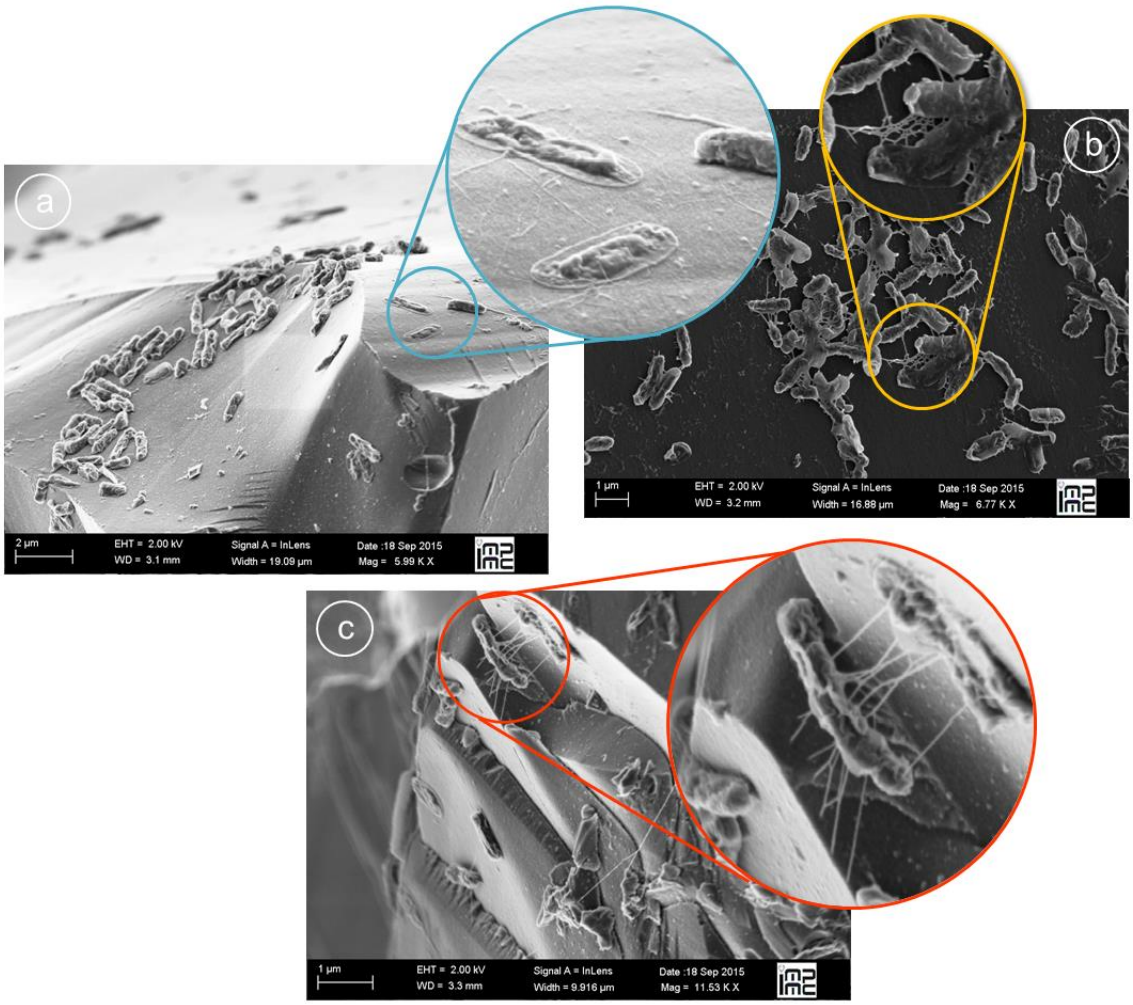

Figure 7: SEM images of the MORB3 glass surface after 15 days of experiments (without dialysis bags).

If bacteria do not seem to massively colonize the surface, they are however homogenously present on the glass grains. The images show that the cells are strongly attached to the glass, as dead cell residues remain at the surface after the CPD protocol (Figure 7a). They also show that biofilm communities start to develop: bacteria produce filamentous structures that allow them to progressively connect to each other (Figure 5b) and to the surface of the glass (Figure 7c). Very similar biofilm patterns were presented in the work on *Pseudomonas stutzeri* of Sudek et al. (2017) between 4 and 7 days of incubation with basaltic glass samples.

Impact on dissolution kinetics

Apparent dissolution rates calculated in abiotic control experiments and in *P. aeruginosa* (with glass confinement or not) based on Si, Al and Fe concentrations measured in the liquid medium are plotted in Figure 8. As free pyoverdine molecules are fluorescent and the formation of complexes between pyoverdine and Fe^{3+} cations is known to induce fluorescence quenching (Albrecht-Gary et al., 1994), the color of the medium after 6 days of experiments is visually represented on the graphics in order to

help the reader to remember the pyoverdine production in each biotic system and its possible interactions with Fe.

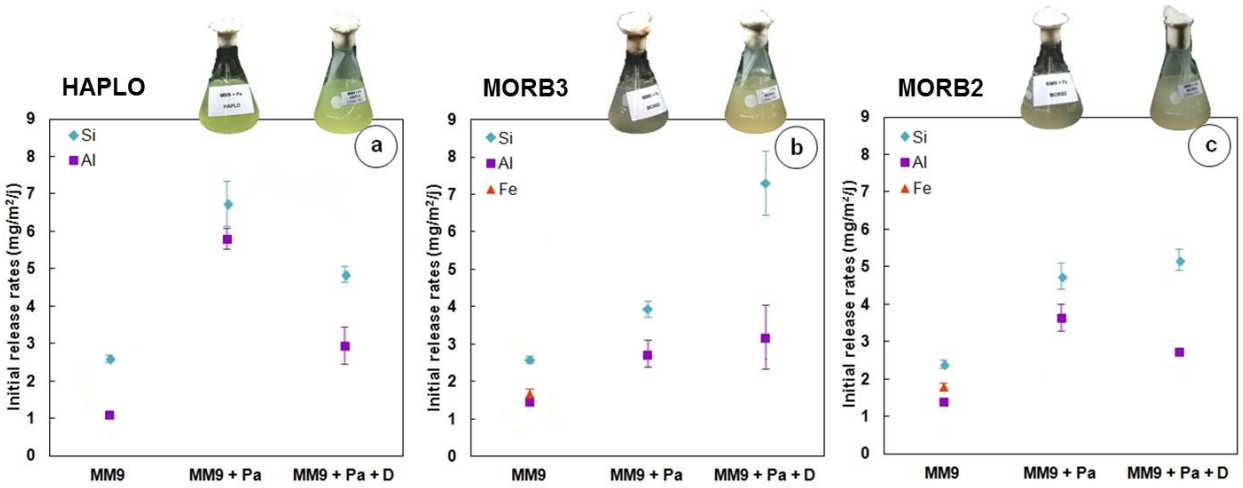

Figure 8: Initial release rates of the HAPLO (a), MORB3 (b) and MORB2 (c) glass confined in dialysis bags and immersed in *P. aeruginosa* culture (MM9 + Pa + D) in comparison with initial rates determined in sterile MM9 and in *P. aeruginosa* cultures (MM9 + Pa) (Perez et al., 2016). The rates were calculated using the average of NL values for both sets of duplicates experiments. Error bars are equal to ± 2SD.

Considering that a fraction of dissolved Al or Fe from the glasses is likely to be trapped within the bacterial cells or adsorbed at their surface (and in consequence not taken in account by ICP-OES measurements), the dissolution rates of the three glasses will be mainly discussed on the basis on Si data.

First of all, the presence of bacterial life in the aqueous medium (MM9) has a positive impact on the global dissolution of the three glasses: the Si release rates are enhanced by a factor of 1.5 to 3 depending on the experimental conditions, whether the glasses are contained in dialysis bag or not.

The dissolution rates calculated from Si concentration of the three glasses are enhanced by comparison with abiotic systems in the order: MORB3 < MORB2 ≈ MORB2-dialysis < HAPLO-dialysis < HAPLO < MORB3-dialysis.

All these results show that:

1/ the presence of pyoverdine molecules has the most significant catalyzing effect on the dissolution. This effect is notably evidenced by the comparison between dialysis and no dialysis-using MORB3 experiments. Without dialysis membranes, the lowest bacterial impact on the dissolution kinetics among all the tested glasses (4.0 ± 0.2 $mg.m^2.d^{-1}$ for Si, Figure 8b) is correlated with the non-detection of pyoverdine in the system (Figure 4). These experiments show that the moderate enhancement relative to the experiment without bacteria is caused by a direct bacteria/glass interaction. By contrast, the dialysis-membrane-using experiments, in which low but significant amounts of pyoverdine (around 20 µM) are detected in solution, are characterized by the highest Si release rates (7.3 ± 0.8 $mg.m^2.d^{-1}$ for Si, Figure 8b).

2/ the relative effect of pyoverdine correlates well with the complex stability constants of the siderophore with the cations in presence ($K^{Fe^{2+}} < K^{Al^{3+}} < K^{Fe^{3+}}$) (Albrecht-Garyet al., 1994; Chen et al., 1994; Hernlem et al., 1996; Szabo et Karkas, 2011). In particular, the siderophore has the most significant effect on the dissolution rates when the cations that are the most likely to form complexes with it are involved as network-forming elements in the glass structure (Al^{3+}, Fe^{3+}). This confirms that complexation reactions between pyoverdine and structural Al and/or Fe promote the dissolution either by a surface-controlled mechanism (Cocozza et al., 2003) or by increasing the solubility of these metallic elements in solution (Oelkers and Schott, 1998). Such siderophore-promoted dissolution has already been well investigated in studies dedicated to the interactions between desferrioxamine-B and Fe(III)-bearing minerals/glass (Reichard et al., 2005; Wolff-Boenisch and Traina, 2007; Cervini-Silva, 2008; Haack et al., 2008; Dehner et al., 2010; Perez et al., 2015). However, there is only a limited number of existing studies exploring the promotion of mineral/glass dissolution by other siderophores and notably pyoverdine (Ferret et al., 2014; Parello et al., 2016; Perez et al., 2016). The results of this work contribute to show the efficiency of pyoverdine in promoting the dissolution of an Fe(III) or Al(III)-bearing glass. For the MORB2 glass, the very similar results in terms of siderophore production (Figure 4) and dissolution rates (Figure 8) from dialysis-membrane to no dialysis-membrane-using experiments confirm that the bacteria-promoting process mainly takes place in solution. This corroborates what was assessed in a previous study by Perez et al. (2016): during the MORB2 glass dissolution, the release of Fe first as Fe^{2+} cations in solution induces the production of pyoverdine molecules. The Fe^{2+} cations being quickly oxidized into Fe^{3+} cations in contact with the oxygenated liquid medium are preferentially chelated by the pyoverdine molecules. Although the change of Fe speciation in solution favors the release of Fe^{2+}, its structural role (network-modifier cation) can explain the lower impact of this preferential release on the global dissolution kinetics of the glass.

3/ the correlation between the effect of pyoverdine on the dissolution kinetics and the complex stability constants does not seem to depend on the concentrations of pyoverdine in the systems. As an example, pyoverdine has the highest impact on dissolution rates of the MORB3 glass with a maximum concentration in the medium equal to 20 µM (Figure 4). By contrast, it has a lower impact on the dissolution kinetics of the HAPLO glass although it is continuously produced by the cells and its concentration approximates 70-80 µM after 6 days of dissolution (Figure 4). Moreover, isolating the HAPLO glass from the bacterial suspension induces a more intense production of pyoverdine (80 µM versus 70 µM) but these experiments are characterized by lower global dissolution rates of the glass (4.9 ± 0.2 $mg.m^2.d^{-1}$ versus 6.8 ± 0.6 $mg.m^2.d^{-1}$ for Si, Figure 8a). These results echoe to several studies evidencing a potential “threshold effect” on dissolution rates concerning the abundance of chelating molecules in solution (Cheah et al., 2003; Wolff-Boenisch and Traina, 2006). A slight decrease in the dissolution rate of basalts was even observed by Neaman et al. (2005) by increasing the concentration of organic ligands in solution.

Conclusion

This work attests of the impact of bacterial life on the dissolution kinetics of three synthetic basaltic model glasses. Isolating the samples from the bacterial suspension was essential to target more precisely the bacterial impact on the dissolution mechanisms/kinetics of basaltic glass and quantifying the different types of bacterial contributions. A direct access to the surface of an Fe(III)-bearing glass is shown to inhibit the production of siderophore by the bacteria and consequently to minimize the bacteria-promoted effect, as the dissolution rates are increased by 1.5 times compared to sterile experiments. By contrast, isolating the glass from the bacterial suspension with dialysis bags triggers the biosynthesis of siderophore, stopped as soon as the bacteria reach a stationary phase of growth. This limited quantity of pyoverdine molecules in solution (around 20 µM) is sufficient to significantly improve the dissolution rate of the MORB3 glass, which is increased by 3 times compared to sterile experiments. By contrast, the dissolution kinetics of an Fe(II)-bearing glass incubated with *P. aeruginosa* are not impacted by the limited access of bacteria to the glass in dialysis experiments: small amounts of siderophore are produced in both cases and the dissolution rate is increased by 2 times compared to sterile experiments. Finally, the Fe-starved bacteria incubated in the presence of the HAPLO glass are shown to continuously produce pyoverdine. As most siderophores, pyoverdine has also a high affinity with Al^{3+} and the dissolution seems to be promoted by the preferential release of Al from the glass induced by the formation of *Al^{3+}-pyoverdine* complexes.

This work is a new contribution regarding the high affinity of microorganisms for basaltic glasses as an Fe-source. In this case Fe is the most likely used by the ferri-reductive model strain *P. aeruginosa* in its Fe^{3+} form as an electron sink. Its quick uptake by *P. aeruginosa* is shown to significantly carry benefit to the growth of the bacteria. Moreover, this study brings new evidences of the positive impact on the dissolution kinetics of these glasses, of the strategies developed by the bacteria to acquire Fe, depending on the form under which it is primarily available to them: 1/ as structural Fe(II) or Fe(III) within the glass network, directly accessible (or not) to them depending on the presence of dialysis-membranes or 2/ in solution first as Fe^{2+} ions or forming soluble complexes with phosphates initially present within the liquid medium. For each Fe source, one bacterial response was identified and each response was shown to impact differently on the dissolution kinetics. Among these bacterial responses, siderophore production was shown to particularly regulate the dissolution rates. In a basaltic environment where Fe solubility is low and where siderophore-producing strains are commonly detected, the biosynthesis of these complexing agents operates as a mechanism developed to ensure nutritional Fe-availability.

Acknowledgements

This work was supported by grants from Region Ile de France and by CNRS-INSU (INTERVIE).

References

Akafia M.M., Harrington J.M., Bargar J.R. and Duckworth O.W. (2014) Metel oxyhydroxide dissolution as promoted by structurally diverse siderophores and oxalate. *Geochim. Cosmochim. Acta* **141**, 258-269.

Ahmed E. and Holmström S. J. M. (2015) Microbe-mineral interactions: The impact of surface attachment on mineral weathering and element selectivity by microorganisms. *Chem. Geol.* **403**, 13-23.

Albrecht-Gary A., Blanc S., Rachel N., Ocaktan A., Mohamed A. and Abdallah A. (1994) Bacterial iron transport: coordination properties of pyoverdine PaA, a peptidic siderophore of *Pseudomonas aeruginosa*. *Inorg. Chem.* **33**, 6391-6402.

Berner R.A., Lasaga A.C., Garrels R.M. (1983) The carbonate-silicate geochemical cycle and its effect on atmospheric carbon dioxide over the past 100 million years. *Am. J. Sci*. **283**, 641-683.

Bray A.W., Oelkers E.H., Bonneville S., Wolff-Boenisch D., Potts N.J., Fones G. and Benning L.G. (2015) The effect of pH, grain size, and organic ligands on biotite weathering rates. *Geochim. Cosmochim. Acta* **164**, 127-145.

Callow B., Falcon-Suarez I., Ahmed S. and Matter J. (2018) Assessing the carbon sequestration potential of basalt using X-ray micro-CT and rock mechanics. *International Journal of Greenhouse Gas Control* **70**, 146-156.

Cheah S., Kraemer S., Cervini-Sila J. and Sposito G. (2003) Steady-state dissolution kinetics of goethite in the presence of desferrioxamine-B and oxalate ligands: implications for the microbial acquisition of iron. *Chem. Geol.* **198**, 63-75.

Cockell C. S. et al. (2010) Microbial endolithic colonization and the geochemical environment in young seafloor basalts. *Chem Geol* **279**, 17–30.

Cocozza C., Tsao C.C.G., Cheah S.F., Kraemer S.M., Raymond K.N., Miano T.M. and Sposito G. (2002) Temperature dependence of goethite dissolution promoted by trihydroxamate siderophores. *Geochim. Cosmochim. Acta* **66**, 431-438.

Cornu J.Y., Huguenot D., Jézéquel K., Lollier M. and Lebeau T. (2017) Bioremediation of copper-contaminated soils by bacteria. *World Journal of Microbiology and Biotechnology* **33**.

Crovisier J., Advocat T. and Dussossoy J.L. (2003) Nature and role of natural alteration gels formed on the surface of ancient volcanic glasses, natural analogs of waste containment glasses. *Journal of Nuclear Materials* **321**, 91-109.

Daux V., Guy C., Advocat T., Crovisier J. L. and Stille P. (1997) Kinetic aspects of basaltic glass dissolution at 90°C: role of aqueous silicon and aluminium. *Chem. Geol*. **142**, 109-26.

Dessert C., Dupré B., Gaillardet J., François L.M. and Allègre C.J. (2003) Basalt weathering laws and the impact of basalt weathering on the global carbon cycle. *Chem. Geol.* **202**, 257-273.

Drever J. and Stillings L. (1997) The role of organic acids in mineral weathering. *Colloids and Surfaces* **120**, 167-181.

Ferret C. (2014) Siderophore-promoted dissolution of smectite by fluorescent Pseudomonas. *Environmental Microbiology Reports* **6**, 459-647.

576 Flaathen T., Gislason S. and Oelkers E. (2010) The effect of aqueous sulphate on basaltic glass
577 dissolution rate. *Chem. Geol.* **8**, 345-354.

578 Gislason S. R. and Oelkers E. H. (2003) Mechanism, rates and consequences of basaltic glass
579 dissolution: II. An experimental study of the dissolution rates of basaltic glass as a function of pH and
580 temperature. *Geochim. Cosmochim. Acta* **67**, 3817-3832.

581 Gordon S.J. and Brady P.V. (2002) In situ determination of long-term basaltic glass dissolution in the
582 unsaturated zone. *Chem. Geol.* **190**, 113-122.

583 Guy C. and Schott J. (1989) Multisite surface reaction versus transport control during the
584 hydrolysis of a complex oxide. *Chem. Geol.* **78**, 181-204.
585
586 Hart R. (1970) Chemical exchange between sea water and deep ocean basalts. *Earth Planet Sci Lett*
587 **9**, 269–279.
588
589 Henri P., Rommevaux-Jestin C., Lesongeur F. and Ménez B. (2016) Structural iron (II) of basaltic
590 glass as an energy source for Zetaproteobacteria in an Abyssal Plain Environment, off the Mid Atlantic
591 Ridge. *Frontiers in Microbiology* **6**, 1518.

592 Hopf J., Langenhorst F., Pollok K., Merten D. and Kothe E. (2009) Influence of microorganisms on
593 biotite dissolution: an experimental approach. *Chemie der Erde – Geochemistry* **69**, 45-56.

594 Hutchens E. (2009) Microbial selectivity on mineral surfaces: possible implications for weathering
595 processes. *Fungal Biology Reviews* **23**, 115-121.
596 Kraemer S., Cheah S., Zapf R., Xu J., Raymond K. and Sposito G. (1999). Effect of hydroxamate
597 sidérophores on Pb(II) adsorption and Fe release from goethite. *Geochim. Cosmochim. Acta* **63**, 3003-
598 3008.
599
600 Lazo D.E., Dyer L.G. and Alorro R.D. (2017) Silicate, phosphate and carbonate mineral dissolution
601 behavior in the presence of organic acids: a review. *Mineral Engineering* **100**, 115-123.

602 Liermann L. J., Kalinowski B. E., Brantley S. L. and Ferry J. G. (2000) Role of bacterial siderophores in
603 dissolution of hornblende. *Geochim. Cosmochim. Acta* **64**, 587-602.

604 Martinez-Luevanos A., Rodriguez-Delgado M., Uribe-Salas A., Carillo-Pedroza F. and Osuna-Alarcon
605 J. (2011) Leaching kinetics of iron from low grade kaolin by oxalic acid solutions. *Applied Clay Science*
606 **51**, 473-477.

607 Mason O., Di Meo-Savoie C., van Nostrand J., Zhou J., Fisk M. and Giovannoni J. (2009) Prokaryotic
608 diversity, distribution and insights into their role in biogeochemical cycling in marine basalts, *ISME J* **2**,
609 231-242.

610 Meyer J. M. and Abdallah M. A. (1978) The fluorescent pigment of *Pseudomonas fluorescens*:
611 biosynthesis, purification and physicochemical properties. *J. Gen. Microbiol.* **107**, 319-328.

612 Morin G.P., Vigier N., Verney-Carron A. (2015) Enhanced dissolution of basaltic glass in brackish
613 waters: Impact on biochemical cycles. *Earth and Planetary Science Letters* **417**, 1-8.

614 Oelkers E. (2001) General kinetic description of multioxide silicate mineral and glass dissolution.
615 *Geochim. Cosmochim. Acta* **65**, 3703-3719.

616 Oelkers E. H. and Gislason S. R. (2001) The mechanism, rates and consequences of basaltic glass
617 dissolution: I. An experimental study of the dissolution rates of basaltic glass as a function of aqueous
618 Al, Si and oxalic acid concentration at 25°C and pH 3 and 11. *Geochim. Cosmochim. Acta* **65**, 3671-
619 3681.

620 Oelkers E. and Schott, J. (1998) Does organic acid adsorption affect alkali feldspar dissolution rates?
621 *Chem. geol.* **151,** 235-245.
622
623 Olsen A. and Rimstidt D. (2008) Oxalate-promoted forsterite dissolution at low pH. *Geochim.*
624 *Cosmochim. Acta* **72,** 1758-1766.
625
626 Orcutt B., Sylvan J., Knab N. and Edwards K. (2011) Microbial ecology of the dark ocean above, at
627 and below the seafloor. *Microbiology and Molecular Biology Review* **75**, 361-422.
628
629 Parrello D., Zegeye A., Mustin C. and Billard P. (2016) Siderophore-mediated iron dissolution from
630 nontronites is controlled by mineral cristallochemistry. *Front. Microbiol.* **7**, Article 423.
631
632 Parruzot B., Jollivet P., Rébiscoul D. and Gin S. (2015) Long-term alteration of basaltic glass :
633 Mechanisms and rates. *Geochim. Cosmochim. Acta* **154**, 28-48.
634 Techer I., Advocat T., Lancelot J. and Liotard J. (2000) Basaltic glass : Alteration mechanisms and
635 analogy with nuclear waste glasses. *J. Nucl. Mater.* **282**, 40-46.

636 Perez A., Rossano S., Trcera N., Verney-Carron A., Huguenot D., van Hullebusch E. D., Catillon G.,
637 Razafitianamaharavo A. and Guyot F., (2015) Impact of iron chelators on short-term dissolution of
638 basaltic glass. *Geochim. Cosmochim. Acta* **162**, 83-98.

639 Perez A., Rossano S., Trcera N., Huguenot D., Fourdrin C., Verney-Carron A., van Hullebusch E. and
640 Guyot F. (2016) Bioalteration of synthetic Fe(III)-, Fe(II)-bearing basaltic glasses and Fe-free glass in
641 the presence of the heterotrophic bacteria strain *Pseudomonas aeruginosa*: impact of siderophores.
642 *Geochimica et Cosmochimica Acta* **188**, 147-162.
643
644
645 Santelli C., Edgcomb V., Bach W. and Edwards K. (2009) The diversity and abundance of bacteria
646 inhabiting seafloor lavas positively correlates with rock alteration. *Environmental Microbiology* **11**, 86-
647 98.

648 Schalk IJ and Guillon L (2013) Fate of ferrisiderophores after import across bacterial outer
649 membranes: different iron release strategies are observed in the cytoplasm or periplasm depending on
650 the siderophore pathways. *Amino Acids* **44**, 1267-1277.

651 Shirokova L. S., Bénézeth P., Pokrovsky O. S., Gerard E., Menez B. and Alfredsson H. (2012) Effect
652 of the heterotrophic bacterium *Pseudomonas reactans* on olivine dissolution kinetics and implications
653 dor CO_2 storage in basalts. *Geochim. Cosmochim. Acta* **80**, 30–35.

654 Schwyn B. and Neilands J. B. (1987) Universal Chemical-Assay for the Detection and Determination
655 of Siderophores. *Anal. Biochem*. **160** 47–56.

656 Spivack A. J. and Staudigel H (1994) Low-temperature alteration of the upper oceanic crust and the
657 alkalinity budget of seawater. *Chem Geol* **115**, 239–247.

658 Staudigel H., Hart S.R. (1983) Alteration of basaltic glass: mechanisms and significance for the
659 oceanic crust seawater budget. *Geochim. Cosmochim. Acta* **47**, 337–350.

660 Stillings L. L., Drever J.I., Brantley S. L and Sun Y. (1995) Rates of feldspars dissolution at pH 3-7 with
661 0-8 mM oxalic acid. *Chem. geol.* **132**, 79-89.

662 Stockmann G. J., Shirokova L. S., Pokrovsky O. S., Bénézeth P., Bovet N., Gislason S. R. and
663 Oelkers E. H. (2012) Does the presence of heterotrophic bacterium *Pseudomonas reactans* affect
664 basaltic glass dissolution rates? *Chem. geol.* **296-297**, 1-18.
665
666 Stroncik N. and Schmincke H. (2001) Evolution of palagonite : Crystallization, chemical changes, and
667 element budget. *Geochem. Geophy. Geosy.* **2**, 365-370.
668

669 Sudek L.A., Templeton A.S., Tebo B.M. and Staudigel H. (2009). Microbial ecology of Fe(hydroxide)
670 mats and basaltic rock from Vailulu'u Seamount, American Samoa. *Geomicrobiol. J.* **26**, 581-596.
671
672 Sudek L.A., Wanger G., Templeton A.S., Staudigel H. and Tebo B.M. (2017) Submarine Basaltic glass
673 colonization by the heterotrophic Fe(II)-oxidizing and siderophore-producing deep-sea bacterium
674 Pseudomonas stutzeri VS-10: The potential role of basalt in enhancing growth. *Front. Microbiol*.

675 Sverdrup H. (2009) Chemical weathering of soil minerals and the role of biological processes. *Fungal*
676 *Biology Reviews* **23**, 94-100.

677 Techer I., Lancelot J., Clauer N., Liotard J. and Advocat T. (2001b) Alteration of a basaltic glass in an
678 argillaceous medium : The Salagou dike of the Lodève Permian Basin (France). Analogy with an
679 underground nuclear waste repository. *Geochim. Cosmochim. Acta* **65**,1071-1086.
680
681 Templeton A. S., Staudigel H. and Tebo B. M. (2005) Diverse Mn(II)-Oxidizing Bacteria Isolated from
682 Submarine Basalts at Loihi Seamount. *Geomicrobiol* **22**, 127–139.

683 Thorseth I., Torsvik T., Torsvik V., Daae F. and Pedersen R. (2001) Diversity of life in ocean floor
684 basalt. *Earth and Planetary Science Letters* **194**, 31-37.
685
686 Torres M.A., West A.J. and Nealson K. (2014) Microbial acceleration of olivine dissolution via
687 siderophore production. *Procedia Earth and Planetary Science* **10**, 118-122.
688
689 Ullman W. J., Kirchman D. L., Welch S. A. and Vandevivere P. (1996) Laboratory evidence for
690 microbially mediated silicate mineral dissolution in nature. *Chem. Geol.* **132**, 11-17.

691 Verney-Carron A., Viguier N. and Millot R. (2011) Experimental determination of the role of diffusion
692 on Li isotope fractionation during basaltic glass weathering. *Geochim. Cosmochim. Acta* **75**, 3452-
693 3468.

694 Wang Q., Gao S., Ma X., Mao X., He L. and Sheng X. (2018) Distinct mineral weathering effectiveness
695 and metabolic activity between mineral-weathering bacteria Burkholderia metallica F22 and
696 Burkholderia phytofirmans G34. *Chemical Geology*, in press.

697 Wang X., Li Q., Hu H., Zhang T. and Zhou Y. (2005) Dissolution of kaolinite induced by citric, oxalic
698 and malic acids. *Journal of Colloids and Interface Sciences* **290**, 481-488.

699 Watteau F. and Berthelin J. (1994) Microbial dissolution of iron and aluminium from soil minerals:
700 Efficiency and specificity of hydroxamate sidérophores compared to aliphatic acids. *Soil Biology* **30**, 1-
701 9.

702 Welch S. and Ullman W. (1992) The effect of organic acids on plagioclase dissolution rates and
703 stoichiometry. *Geochim. Cosmochim. Acta* **57**, 2725-2736.

704
705 Wolff-Boenisch D., Gislason S. R., Oelkers E. H., and Putnis C. V. (2004a) The dissolution rates of
706 natural glasses as a function of their composition at pH 4 and 10.6, and temperatures from 25 to
707 74°C.*Geochim. Cosmochim. Acta* **68**(23), 4843-4858.

708 Wolff-Boenisch D., Gislason S.R. and Oelkers E.H. (2004b) The effect of fluoride on the dissolution
709 rates of natural glasses at pH 4 and 25°C. *Geochim. Cosmochim. Acta* **68**, 4571-4582.

710 Wolff-Boenisch D. and Traina S.J. (2007) The effect of desferrioxamine B, enterobactin, oxalic acid,
711 and Na-alginate on the dissolution of uranyl-treated goethite at pH 6 and 25°C. *Chem. Geol.* **243**, 357-
712 368.

713 Wolff-Boenisch D., Wenau S., Gislason S. R. and Oelkers E. H. (2011) Dissolution of basalts and
714 peridotite in seawater, in the presence of ligands, and CO_2: implications for mineral sequestration of
715 carbon dioxide. *Geochim. Cosmochim. Acta* **75**, 5510-5525.

716